

Review

Viral ion channels: structure and function

Wolfgang B. Fischer^{a,*}, Mark S.P. Sansom^b^a Department of Biochemistry, University of Oxford, South Parks Road, Oxford OX1 3QU, UK^b Laboratory of Molecular Biophysics, Department of Biochemistry, University of Oxford, South Parks Road, Oxford OX1 3QU, UK

Received 10 February 2001; received in revised form 30 October 2001; accepted 22 November 2001

Abstract

Viral ion channels are short auxiliary membrane proteins with a length of ca. 100 amino acids. They are found in enveloped viruses from influenza A, influenza B and influenza C (Orthomyxoviridae), and the human immunodeficiency virus type 1 (HIV-1, Retroviridae). The channels are called M2 (influenza A), NB (influenza B), CM2 (influenza C) and Vpu (HIV-1). Recently, in *Paramecium bursaria chlorella* virus (PBCV-1, Phycodnaviridae), a K⁺ selective ion channel has been discovered. The viral channels form homo oligomers to allow an ion flux and represent miniaturised systems. Proton conductivity of M2 is established; NB, Vpu and the potassium channel from PBC-1 conduct ions; for CM2 ion conductivity is still under proof. This review summarises the current knowledge of these short viral membrane proteins. Their discovery is outlined and experimental evidence for their structure and function is discussed. Studies using computational methods are presented as well as investigations of drug–protein interactions. © 2002 Elsevier Science B.V. All rights reserved.

Keywords: Viral ion channels; Influenza; HIV-1; Structure and function; Computational methods; Drug-protein interactions

1. Introduction

Ion channels are membrane spanning proteins which allow an ion flux across the cell membrane by forming internal water filled pores [1]. Ion channels may be formed from the assembly of short peptides just long enough to span the lipid bilayer once, such as the anti-microbial alamethicin (19 amino acids) [2]. They can also be formed by even shorter peptides, such as for example gramicidin (15 amino acids) [2], which have to form dimers to fully transverse the bilayer. Ion channels are also found that consist of several subunits each built up by several

hundreds of amino acids (e.g. the nicotinic acetylcholine receptor has ca. 500 amino acids per subunit [3–7]). However, in this case the assembly of subunits to homo or hetero oligomers is an essential pre-requisite for the creation of water filled pores. The overall nomenclature of the larger channels is related either to the high selectivity to conduct particular ions (e.g. K⁺-, Na⁺-, and Ca²⁺-channels) or to the ligand which induces the function (e.g. acetylcholine for nicotinic acetylcholine receptor, glycine for glycine receptor). Usually, all the ion channels mentioned above conduct at least one of the physiological relevant ions such as Na⁺, K⁺, Ca²⁺, Cl[−] and H⁺.

1.1. Discovery of the viral channel proteins and their roles in the life cycle of the viruses

In the last two decades quite short auxiliary pro-

* Corresponding author. Fax: +44-1865-275234.

E-mail address: wolfgang.fischer@bioch.ox.ac.uk (W.B. Fischer).

teins with a length of ca. 100 amino acids have been found in enveloped viruses from influenza A [8–10], influenza B [11,12], and influenza C [13] (Orthomyxoviridae), and in the human immunodeficiency virus type 1 (HIV-1, Retroviridae) [14,15] (Fig. 1). Recently, in chlorella plant virus PBCV-1 (Phycodnaviridae), a highly K^+ selective ion channel has been discovered that is 94 amino acids long [16] (Fig. 1). Ion channels like nAChR or KcsA are, respectively, ca. five times and one third bigger than the viral channels. The viral channels therefore represent miniaturised channel systems.

The channel protein M2 from influenza A exhibits proton conductance. According to the overall similarity in the viral life cycles and the homology in length it is suggested that the short auxiliary proteins NB (from influenza B), CM2 (from influenza C) and Vpu (from HIV-1), share similar roles and function in the life cycles of their viruses.

Influenza A viruses, like other enveloped viruses, enter the host by attaching to the host cell's membrane. As a consequence the host incorporates this section of the cell membrane until this section is finally tied off forming a 'vesicle' (endosome) with the virion included. This type of entry is called the endocytotic pathway. Once caged in the endosome the host cell starts acidifying this compartment via ATPases. The virions have to escape from this dangerous

environment. In a narrow range of pH, 5.0 to 5.5 in the case of influenza A, fusion of the viral membrane with the cell membrane of the endosome is facilitated (see 1–4 in [17]). Membrane fusion is triggered by conformational changes of the membrane protein hemagglutinin, a consequence of lowering the pH [17]. Also the release of the virus' RNA into the host cell is enabled by the low pH. The viral membrane protein M2 is found to be responsible for changing the pH in the interior of the virion. It is encoded in the RNA segment 7 of influenza A [10,18]. The M2 mediated change of pH is found to be induced by the formation of a homo tetrameric assembly forming a proton conducting channel [19–22]. M2, transcribed in the infected cell, is also responsible for the proper structure of hemagglutinin in the later stage of the viral life cycle [23]. Experiments with amantadine, which blocks M2 channel activity, have shown that without the function of M2, hemagglutinin is found at the cell surface in its low pH structure [24]. Viruses with wild type M2 and M2 mutants resistant to amantadine do not show hemagglutinin in its high pH conformation at this later stage of the viral life cycle. Consequently M2 is also effective at the end of the viral life cycle by retaining a high pH in cellular subcompartments.

For NB and CM2 the exact role in the life cycles of the viruses is not yet identified. By analogy with

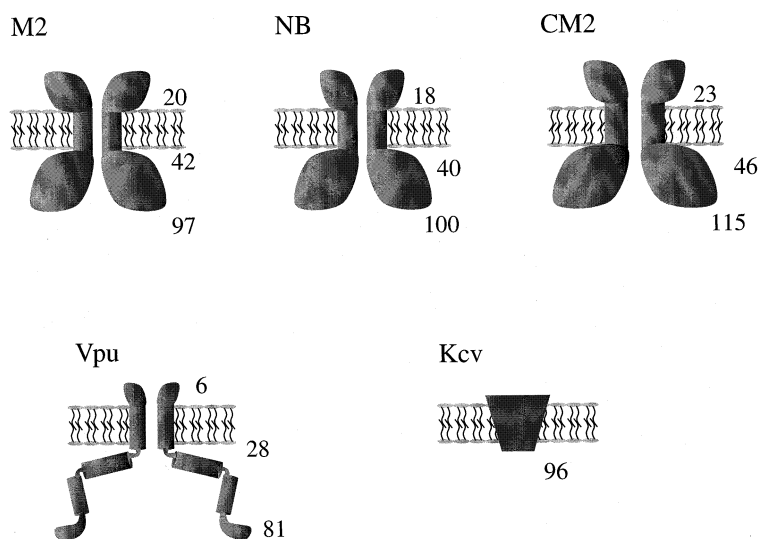


Fig. 1. Assumed topology of the putative viral ion channel proteins. Numbers indicate the amino acids which mark the beginning and the end of the TM segment, and the total number of amino acids. The rods for Vpu indicate helical segments which are found by experimental methods.

M2 it is suggested that NB may also have a role in virus entry [25,26].

Vpu is expressed in the membranes of subcellular units of infected cells and is not found in the membrane envelope of the virion. It has a triple role in the life cycle of HIV-1, for which two distinct parts of the protein are responsible. Vpu increases virus release by triggering a cascade of steps which finally leads to the down-regulation of CD4 protein expression on the surface of the infected cell [27,28]. CD4 protein of the host cell is the receptor to which the virion binds. Vpu binds with its cytoplasmatic domain [29] to amino acids 402 and 420 of CD4 [30]. This leads to a destabilisation of CD4. Consequently the formation of a CD4–gp160 complex is prohibited. This complex would have otherwise been ‘trapped’ in the endoplasmic reticulum. gp160 is an essential precursor of the viral coat proteins gp120 and gp41, and hence must reach the cell membrane if secreted virions are to be functional.

Evidence for a functional role of the transmembrane (TM) domain of Vpu was shown by Schubert et al. [31]. Expression of the TM domain revealed enhanced particle release but showed no effect on CD4 degradation. Expression of the Vpu with a ‘scrambled’ TM sequence still induced CD4 degradation but was unable to enhance the release of the virions. Deletion of several amino acids at both the N- and C-terminal ends also leads to protein which is not able to support particle release [32].

Recently it has been found that the down-regulation of major histocompatibility complex 1 in the infected cell is accompanied by the presence of Vpu [33].

Sequence analysis of the double-stranded DNA of PBCV-1 revealed a 94-codon open reading frame that resembles the motif of the pore domain of potassium channels. Experimental data about the exact role during the viral life cycle have not yet emerged. One might conclude that the channel retains or modifies electrochemical gradients in cellular subcompartments or the virion itself.

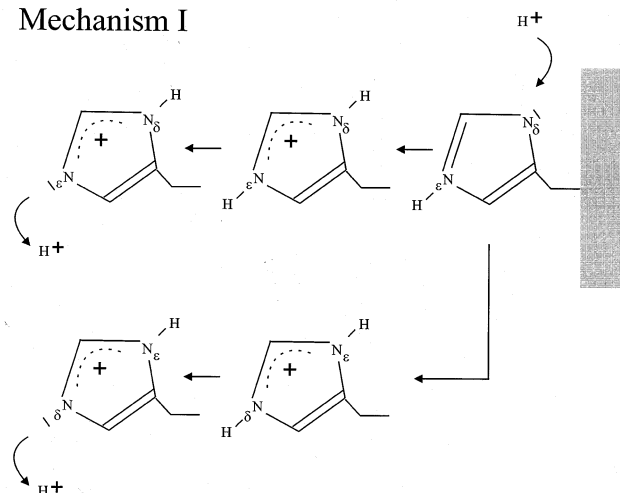
1.2. Channel formation and gating of ion channels

M2 from influenza A has a single TM segment which crosses the bilayer. Pores are formed by the assembly of two homodimers linked via disulfide

bridges [19–22]. The number of segments forming the pore derive from M2 protein expressed in embryonated eggs purified by non-reducing sodium dodecyl sulphate–polyacrylamide gel electrophoresis (SDS–PAGE) analysis. With this method proteins are separated according to their molecular weight. However, whether the number of segments is the same in all membranes of cellular subcompartments of the infected cell is not yet specified. This stands also for all other viral ion channel proteins. The structural motif of the TM segment is an α -helix. Also, in receptors and channels (e.g. nAChR, glycine receptor) assemblies of single helices form the pore across the membrane [34]. They are slightly kinked about midway through the pore and surrounded mostly by at least two more helices in each of the five subunits.

For M2 of influenza A, histidine-37 has been found to be involved in pH induced channel opening

Mechanism I



Mechanism II

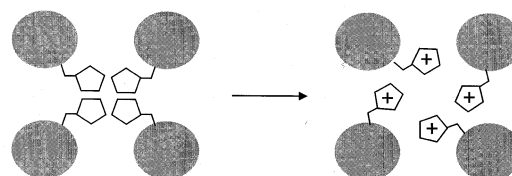


Fig. 2. Proposed gating mechanisms for M2 from influenza A. Top: mechanism I: tautomerisation or ‘flipping histidine rings’. Bottom: mechanism II: ‘swinging doors’. Picture adopted from [105].

[35]. Two possible gating mechanisms are presently discussed in the literature: (i) a tautomerisation or ‘flipping of the histidine rings’ (channel blocking, mechanism I) [36], and (ii) swinging doors (gating, mechanism II) involving electrostatic repulsion [37] (Fig. 2). In mechanism I, one of the two nitrogens in the histidine ring system is protonated by the low pH and consequently the side-chain flips around its C α –C β bond due to the energetic state of the two nitrogens. Additional protons on the ‘low pH’ side attach to the ‘proton-free’ nitrogen thereby releasing the proton of the other nitrogen which is now on the high pH side. Mechanism II (Fig. 2) assumes that there is an increased probability of the histidine ring becoming doubly protonated at low pH. Consequently, a positive charge emerges which leads to a repulsion of the histidines. This repulsion forces the histidines towards the helix–helix interface, with a possible rotational motion of the entire helix.

For the other channel proteins exact gating mechanisms have not yet emerged.

1.3. Anti-viral drugs affecting channel activity of M2

Until recently the only anti-viral drug available was amantadine. Amantadine selectively interacts with the channel protein M2 from influenza A in concentrations below 1 μ M [38–41]. Interaction with all other channel proteins needs drastically higher concentrations. This makes amantadine applicable for medical treatment only against influenza A. There are still ongoing investigations regarding the discovery of novel anti-viral drugs attacking the channel proteins [42].

2. Experimental analysis

The most important achievement in protein research is to provide a structural and functional model of the desired protein, and this down to an atomic resolution (<2 Å). This would create an essential platform for further biophysical studies on the protein. It would also serve the demands for more focussed screening of potential drugs. In the case of the viral ion channels any structural model of the full length proteins delivered either by X-ray or nuclear magnetic resonance (NMR) spectroscopy is still lack-

ing. This is in common with most of the other larger ion channel proteins, except for the bacterial K⁺-channel [43]. Nevertheless, there have been excellent efforts to deliver ‘indirect’ structural data of the structure and function of these proteins with a variety of methods from the fields of molecular biology, electrophysiology and spectroscopy (NMR, circular dichroism (CD), Fourier transform infrared (FTIR) spectroscopy), including computational methods such as molecular dynamics (MD) simulations. In this section we will provide results and their interpretation of the viral ion channel proteins. The results of the MD simulations will be discussed in more detail in Section 3.

2.1. Sequence and topology of putative ion channel proteins: M2, NB, CM2, Vpu, Kcv

The putative viral ion channels M2, NB, CM2, Vpu and Kcv do not show any sequence homology (Fig. 3). M2, NB, CM2 and Vpu have in common a sequence of ca. 22–26 amino acids with a high content of hydrophobic residues. This consequently suggests that the proteins span the bilayer only once. The loci of the TM segment is almost in the middle of the complete sequence for M2, NB, and CM2 (Fig. 3) and close to the N-terminal (N) end for Vpu. CM2 and Vpu are both type I membrane proteins with a cleavable signal peptide (secretory signal peptide) according to von Heijne [44]. This results in a N_{out}–C_{in} topology (C: C-terminal end). M2, NB and Kcv have in common a type III membrane protein topology with uncleaved N-terminal ‘start–stop’ signals which penetrates the membrane and generates a N_{out}–C_{in} topology (according to von Heijne). For completion: type II proteins have uncleaved ‘start–stop’ signals (starts or stops protein production) leading to a N_{in}–C_{out} topology.

So far the best characterised protein is M2 [45] (Table 1). Its sequence of 97 amino acids is encoded on the RNA segment 7 [46,47]. The molecular weight of M2 is ca. 15 kDa [46,48]. It has a single phosphorylation site at serine residue 64 [20,49]. SDS–PAGE analysis following a treatment of the immunoprecipitate with reducing agents revealed that the monomers are held together via cysteines at position 17 and 19 [23]. Another cysteine at position 50 is assumed not to contribute to the linkage of the sub-

M2 Weybridge (P05778)						
MSLLTEVETP ¹⁰	TRNGWECSCS ²⁰	DSSDPLVIAA ³⁰	<u>SIIGILHFLI</u> ⁴⁰	<u>WILDRLEFFKC</u> ⁵⁰	IYRLKYGLK ⁶⁰	RGPSTEGVPR ⁷⁰
SMREEYRQEQ ⁸⁰	QNAVDVDDGH ⁹⁰	FVNIELE ⁹⁷				
NB (P03493)						
MNNATFNCTN ¹⁰	INPITHIRGS ²⁰	<u>IIITICVSLI</u> ³⁰	<u>VILIVFGCIA</u> ⁴⁰	KIFINKNCT ⁵⁰	NNVIRVHKRI ⁶⁰	KCPDCEPFCN ⁷⁰
KRDDISTPRA ⁸⁰	GVDIPSFILP ⁹⁰	GLNLSEGTEN ¹⁰⁰				
CM2 (Q67392)						
MGRMAMKWL ¹⁰	VIIYFSITSQ ²⁰	PASACNLKTC ³⁰	LNLFNNTDAV ⁴⁰	TVHCFNFTE ⁵⁰	<u>QGYMLTLASL</u> ⁶⁰	<u>GLGIITMLYL</u> ⁷⁰
LVKIIIELVN ⁸⁰	GFVLGRWERW ⁹⁰	CGDIKTIMP ¹⁰⁰	EIDSMKFTD ¹¹⁰	IALFRERLDL ¹²⁰	GEDAPDETND ¹³⁰	SPIPFSDGIF ¹⁴⁰
ET ¹⁴²						
Vpu (P05919)						
QPIPIVAIVA ¹⁰	<u>LVVAIIIAIV</u> ²⁰	<u>VSVIIVIEYR</u> ³⁰	KILRQRKIDR ⁴⁰	LIDRLIERAE ⁵⁰	DSGNESEGET ⁶⁰	SALVEMGVEM ⁷⁰
GHHAPWDVDD ⁸⁰	L ⁸¹					
Kcv [16]						
MLVFSKFLTR ¹⁰	TEPFMIHLFI ²⁰	<u>LAMFVMIYKF</u> ³⁰	<u>FFGGFENNFS</u> ⁴⁰	VANPDKKASW ⁵⁰	IDCIYFGVTT ⁶⁰	<u>HSTVGFGDIL</u> ⁷⁰
PKTIGAKLCT ⁸⁰	<u>IAHIVTVFFI</u> ⁹⁰	<u>VLT</u> ⁹⁴				

Fig. 3. Primary sequences (notation according to SWISS-PROT data bank <http://www.ebi.ac.uk/swisprot/>) of the putative viral ion channel proteins. Bold and underlined: the assumed helical TM spanning segments. For Kcv: bold: selectivity filter motif.

units but is palmitoylated [50,51]. The occurrence of bands corresponding to the molecular weight of ca. 70 kDa in the SDS–PAGE analysis of the immunoprecipitate without using reducing agents indicates the presence of tetramers. For M2 protein at higher concentrations, bands corresponding to a mass of ca. 200 kDa on sucrose gradients also indicate the existence of some kind of superstructure [52,53]. However, the functional stoichiometry is found to be homotetrameric [53] by using the method of MacKinnon [54] with mixed oligomers. M2 comprises of an N-terminal extramembraneous part of 18–23 residues, a TM part of ca. 19 residues, and a C-terminal cytoplasmic part of ca. 54 residues [46,48].

NB is an integral membrane protein of 100 amino acids in length [12] (Table 1). It contains two asparagine residues (3 and 7) which are linked with carbohydrates [55]. In an early stage NB exists as an unglycosylated protein (NB₁₂) with a molar mass of ca. 12 kDa. NB₁₂ can be modified with two high mannose carbohydrate chains into NB₁₅ (15 kDa) and NB₁₈ (18 kDa). Further modification with several lactosaminoglycan generates NB_{pl} with a molar weight of ca. 20–60 kDa. The first 19 amino acids are located at the extramembraneous side, it is suggested that residues 19 to 40 transverse the membrane, while the remaining 60 amino acids are found in the cytoplasm [56].

CM2 (type I) is cleaved from a precursor protein P42 by signal peptidase when oriented in the lipid membrane (Table 1). After cleavage it is left with a length of 115 amino acids [57–59]. In its unglycosy-

lated form CM2 has a molecular weight of ca. 16 kDa [60]. It is post-translationally modified firstly by the addition of high-mannose carbohydrate chains ($M_r \sim 18$ kDa [13]) and then further by polylactosaminoglycans when still within the P42 unit ($M_r \sim 21$ –35 kDa [57]). The carbohydrates are added via the first asparagine residue (Asp-26, Table 1) [58]. The first 23 residues of CM2 are extramembraneous, the consecutive 23 residues are hydrophobic and long enough to span the bilayer. The remaining 69 amino acids are cytoplasmic giving its topology as N_{out}–C_{in} [57]. Non-reducing SDS–PAGE showed that the protein is expressed as disulphide-linked dimers and tetramers [57].

Vpu is a type I integral membrane protein (ca. 16 kDa [14,15]) with a hydrophobic N and a hydrophilic C terminus [61] (Table 1). It has phosphorylation sites at serine residues 52 and 57 [27,62,63]. Chemical cross-linking experiments reveal that Vpu exists as oligomers with approximate weights of 28, 45, 80 and 85 kDa [61]. Oligomerisation is found for membrane-free as well as for membrane-associated Vpu. The presence of CD4 leads to the loss of any oligomeric assembly of Vpu. Experiments with Vpu and Vpu hybrids provides evidence that Vpu self-assembles to form homo oligomers. The exact number of units which forms the assemblies is not known.

Kcv is 94 amino acids long. The hydropathy analysis of Kcv exhibits two hydrophobic TM segments which are separated by a sequence of 44 amino acids [16] (Fig. 3). This sequence contains the TxxTxGFG motif found in K⁺ channels. The primary sequence of Kcv differs markedly from that of the other

Table 1
Properties of the putative viral ion channels

	M2	NB	CM2	Vpu	Kcv[16]
Protein type	III [45]	III [12]	III [58]	I [14, 15]	–
Length (amino acids)	97 [46,47]	100 [12]	115 [57,58]	81 [14,15]	96
Phosphorylation sites	Ser-64 [20,49]	–	–	Ser-52, Ser-56 [27,62,63]	putative residues 9–12 (Tyr-Arg-Tyr-Glu)
Glycosylation sites	palmitoylated at Cys-50 [50,51]	Asp-3, Asp-7 [55].	Asp-26 [13,57,58]	–	–
Putative channel structure	homo-tetramer cysteine-linked [23]	homo-pentamer [132]	homo-tetramer [57]	homo-pentamer [111]	homo-tetramer
Helical structure of solely the TM segment reconstituted in lipid bilayer confirmed by	CD (DOPC) [84], solid state NMR [85–87].	CD [75]	FTIR [90]	FTIR [94] solid state NMR [93,95]	assumed comparable to KcsA from sequence homology
Experimental tilt angle of solely the TM segments	NMR: $33 \pm 3^\circ$ (DMPC) [85] $37 \pm 3^\circ$ (DMPC) [86] FTIR: $31.6 \pm 6.2^\circ$ (DMPC) [88]	–	$14.6 \pm 3.0^\circ$ FTIR [90]	$\sim 6.5^\circ$ (FTIR) [94], $< 30^\circ$ (NMR) [93] $\sim 15^\circ$ solid state NMR [95]	assumed comparable with KcsA
Structure of extramembraneous domains	–	–	–	two to three helical domains; solution NMR [96,97], CD [92]	no domains
Sensitivity to amantadine	0.1–5 μ M, irreversible for M2 protein expressed in oocytes [22], reversible for TM segment [21]	2 mM for NB protein [74] 0.04–0.06 mM TM segment, reversible [120]	–	–	half inhibition by 2 and 0.8 mM, reversible

K⁺ channels. Phylogenetic comparison with selected K⁺ channels (e.g. Kir, Kv, tandem K⁺, eukaryotic and prokaryotic K⁺ channels) suggests that Kcv belongs to an independent cluster. The N-terminal end comprises a phosphorylation site at residues 9 to 12 (Table 1). The hydrophobicity profile proposes TM segments from residues 13–34 and 78–94. The C-terminal end of Kcv is merged with the first TM segment which indicates a missing cytoplasmic domain. Similar to the other viral ion channels, Kcv also is a miniaturised channel system.

2.2. Experimental evidence for ion conductance of viral channel proteins and synthetic TM segments

Experiments with full length M2 expressed in *Xenopus laevis* [22,64] and yeast [40] reveal channel activity in living cells. Channel activity is found for M2 expressed in mammalian cells (CV-1) using the patch clamp technique [65] and for M2 expressed in the

same cell line, but purified and reconstituted into planar lipid bilayers (phosphatidyl serine:phosphatidyl ethanolamine, 1:1) [66]. Channel activity in this work appears in bursts with brief currents as high as 25–500 pS. The lowest conductance states are recorded around 25–90 pS. More recent experiments, with M2 expressed from a recombinant baculovirus in insect cells (*Trichoplusia ni*) purified and reconstituted into liposomes, demonstrate proton currents as small as 1.2 attoampere (aA) at pH ~ 7 and 2.7–4.1 aA at pH 5.7 in a cation translocation fluorescence assay at 18°C [67]. Extrapolation of the data to 37°C would lead to conductance of 0.03 to 0.4 fS. In these experiments proton selectivity is more than 3×10^6 with respect to sodium and potassium. M2's low single channel conductance and high proton selectivity prevents almost any perturbation of ionic gradient whilst active. Experiments show that histidine in the TM region is essential for channel activity [35]. Whole cell recordings with mutants, in

which histidine is replaced by either glycine or lysine, show current insensitive to low pH. Wild-type M2 drastically increases its channel conductance by 30-fold in the same type of experiment.

Proton selectivity of the whole protein is tested with M2 expressed in *Spodoptera frugiperda* Sf9 cells and reconstituted into lipid vesicles (L- α -dimyristoyl phosphatidylcholine (DMPC) and L- α -dimyristoyl phosphatidyl L-serine, 0.85:0.25) using a fluorescence assay [52]. Whole cell recordings with M2 expressed in *X. laevis* are in support of proton selectivity [68]. However, the results are treated with caution. More recent investigations on M2 transcribed in CV-1 cells confirm proton conductivity [69]. Proton conductance is limited when the capacity of the buffer is reduced. Whole cell measurements on oocytes with expressed M2 in a D₂O medium lead to a $\sim 50\%$ decrease of the membrane current. The interpretation of this finding is that the proton does not move as a hydronium ion through the channel [69]. In a recent investigation it is shown by the same group that M2 is also capable of conducting NH₄⁺ [70].

Experiments with a synthetic peptide construct corresponding to the putative TM section of M2 (25 residues) reconstituted in lipid bilayer (palmitoyl-oleoyl phosphatidylethanolamine and palmitoyl-oleoyl phosphatidylserine, 1:1) reveal the existence of proton conducting channels [21]. Single channel recordings are observed with a conductance of ca. 10 pS at a pH of 2.3. Higher values are attributed to multi-channel openings due to a higher peptide concentration. The analysis corresponds to a tetrameric assembly of single TM segments. A tetrameric assembly of the TM segment of M2 (SSDPLVVAA-SIIGILHLILWILDRL) in dodecylphosphocholine (DPC) induced by low pH is supported by findings using analytical ultracentrifugation [71,72].

The relative high conductance of 10 pS compared to the most recent data on full length M2 (0.4 fS) [69] might be due to the fact that the segments self-assemble. Full length M2 strands transcribed in cells are held together by disulfide bridges to form a dimer of a dimer (tetrameric assemble as a functional unit). This linkage might allow for tightly packed channels formed by the TM segments. The exact role of the extramembraneous parts of M2 has therefore to be analysed. Experiments are done with truncated M2 at residue sites 52, 62, and 82 along the cytoplasmic

end showing decreased channel activity [73]. This study shows that the C-terminal end is essential for stabilising the ‘open state’ of the channel. It would be of extreme interest to know whether these truncations affect the orientation of the TM segments in respect to the membrane normal.

According to homology in topology (a 19-amino-acid-long highly hydrophobic segment) NB is expected also to form proton or ion channels. Experiments with NB transcribed in *Escherichia coli* and reconstituted in a mixture of lipids (palmitoyl-oleoyl-phosphatidylethanolamine, palmitoyl-oleoyl-phosphatidylserine and palmitoyl-oleoyl-phosphatidylcholine, 5:3:2) reveal channel activity [74]. H⁺ conductivity is questioned but not excluded by a series of experiments using glycine-HCl and glycine-H₂SO₄. Channel activity at pH 2.5 could be attributed to Cl[−] ions. At neutral pH NB forms slightly cation selective channels ($P_{\text{Na}}/P_{\text{Cl}} \sim 9$) whereas at a pH of 2.5 the channel turns to become chloride selective ($P_{\text{Cl}}/P_{\text{Na}} \sim 4$). However, conductance of protons at neutral pH is not completely ruled out by the authors, but proton conductance is smaller than the sodium conductance. The overall conductance level at neutral pH is 45 pS when the protein is directly incorporated into the lipid bilayer. Experiments with NB pre-reconstituted into liposomes and consequently added to the *cis* chamber of the sample holder show conductance as small as 10 pS at low NB concentration. With the same method, conductance as high as several hundred pS are observed at higher NB concentration due to the simultaneous opening of several channels. These results suggest that ca. 10 pS reflects the lowest single conductance level observed for NB. This level is similar to those found for the TM segment of influenza A’s M2 in an artificial bilayer [21]. The higher values also could be due to simultaneous activity of multiple channels [21,66]. Experiments with the TM segment of NB reconstituted into a lipid bilayer (1,2-diphtanoyl-3-*sn*-phosphatidylcholine (POPC)) reveal conductance levels of ca. 20, 61, 107 and 142 pS in 0.5 M KCl buffer solution [75].

For CM2 no data are available to prove channel activity of the protein.

Channel activity of Vpu is proved by reconstitution of the whole protein into planar lipid bilayers [76]. For this study, Vpu is transcribed in *E. coli* and purified. Reconstitution has been done either from a

detergent solution or from a suspension of Vpu-containing vesicles. It could be shown that Vpu channel activity is more in preference of monovalent cations than anions. Currents of up to 2 pA (−80 mV) in a 0.5/0.05 M NaCl solution have been recorded. Reconstitution into a lipid membrane of a synthetic analogous to the TM region of Vpu shows channel activity of up to 60 pS with a preference to monovalent cations [29]. A peptide of the same length with a scrambled sequence does not exhibit any channel activity.

Whole cell currents under voltage clamp conditions of the complete Vpu protein in the cell membrane of infected *Xenopus* oocyte cells is also found with a slight preference to monovalent cations [29]. Infection of cells with cRNA encoding for Vpu and having both phosphorylation sites mutated (Ser to Asp) show much higher membrane currents than cells infected with Vpu which has the intact sequence. Voltage clamp recordings of *Xenopus* oocytes infected with Vpu genes do not show any increase in TM currents [77]. To summarise, Vpu is not expressed at the cell surface.

The experiments mentioned are in favour of channel activity of the full length Vpu. However, experiments with any kind of blockers are still lacking and would be the final verification of ion channel properties of Vpu [78]. Experiments with Vpu expressed in amphibian oocytes even question direct channel activity [77]. It is instead suggested that Vpu alters membrane potential by destabilising host cell membrane proteins. However, recent experiments with amiloride derivatives show blocking of channel activity of a peptide analogous to the TM segment of Vpu and full length Vpu both reconstituted in lipid membranes (Ewart et al., early online publication in *Eur. Biophys. J.* (2001), <http://link.springer.de/link/service/journals/00249/tocs.htm>). The authors have also shown reduced virus-like particle release from HeLa cells in the presence of amiloride derivatives with electron microscopy.

Kcv function is determined by expressing the protein in *Xenopus* oocytes [16]. Voltage clamp recordings show differences to control oocytes. The mRNA-injected oocytes exhibit currents up to 10 μ A depending on experimental conditions. Ion selectivity shows a preference for K^+ rather than Na^+ ions with a ratio of $P_K/P_{Na} = 9.32$.

2.3. Comparison of conductance data with those from other ion channels and channel peptides

Viral ion channel forming peptides analogous to the TM segment of M2, NB and Vpu allow for currents for putative single channels of 10–90 pS. Also full length NB, Vpu and Kcv operate in the same range. This is in accord with findings on much larger ion channels such as the receptors (nicotinic acetylcholine, glutamate, glycine and GABA receptors) and voltage gated ion channels (Na^+ -, K^+ -, and Ca^{2+} -channels) ([1], ch. 12, pp. 315–336). For the receptors mainly residues such as aspartic and glutamic acids, glutamines, serines and threonines are pore lining residues. Purely TM peptides like, for example, δ -toxin from *Staphylococcus aureus* [79] exhibit conductances around 70 and 100 pS at low peptide concentration and a conductance of ca. 450 pS at higher concentrations [80]. Also, synthetic peptides based on almost the same alternating hydrophilic/hydrophobic residues lining the pore, e.g. $H_2N-(LSSLLSL)_3-CONH_2$ [81], do show ion channel activity with conductance around 70 pS in a 0.5 M KCl solution. Mellitin, an amphiphilic peptide with largely hydrophobic residues lining the pore and some hydrophilic residues at the C-terminal end also show conductance of ca. 110 pS in 1.8 M NaCl. In contrast, alamethicin has purely hydrophobic pore lining residues [2]. In a planar lipid bilayer the peptide produces several conductance levels. We obtained currents of ca. 100, 310, 690 and 1180 pS (Fischer and Sansom, data not shown) at concentrations of around 0.5 μ M alamethicin [82,83]. Small pores (< 6 segments) of alamethicin still show quite high conductance levels. The hydrophobic walls of a pore wide enough to allow for a uniform water filled channel strongly enhance the diffusion of the ions through the pore. However, once hydrophilic residues line the pore the particular type and sequence of hydrophilic amino acid within the pore might not be of much relevance for generating the conductance values. Instead, they seem to produce potential surfaces for ion permeation.

The most recent results on full length M2 of about 0.4 fS [69] suggest that in the case of the viral M2 channel the extramembraneous and cytoplasmic domains are tightening the segments together forming the proper environment for proton translocation. It will be extremely important to conduct similar ex-

periments as in [69] with the other viral channel proteins with and without their non-TM domains.

2.4. Structural models of the viral channel proteins derived from NMR, FTIR and CD spectroscopy

CD spectroscopy has given first evidence that the TM part of M2 is helical [84] (Table 1). A synthetic analogue corresponding to the predicted TM part of M2 (SSDPLVVAASIIGILHLILWILDRL) is synthesised and reconstituted in 1,2-dioleoyl-*sn*-glycero-3-phosphocholine (DOPC). Solid state NMR spectroscopy is used to evaluate the orientation of the helix in the lipid membrane [85]. Five samples, each single site labelled with ^{15}N on the TM isoleucines 32, 33, 35, 39 and 42, are reconstituted in DMPC vesicles. The results showed a uniform α -helix along the TM segment (SSAPLVVAASIIGILHLILWILDRL) adopting a tilt angle of $33 \pm 3^\circ$ with respect to the membrane normal. Changing the thickness of the bilayer does not result in a remarkable change in the tilt angle of M2 ($37 \pm 3^\circ$ in DMPC, $33 \pm 3^\circ$ in DOPC) [86]. Refinement of the NMR spectroscopic investigations using solid state ^{15}N polarisation inversion spin exchange at magic angle confirms the finding of the tilt angle around 32 – 38° [87]. Site directed infrared dichroism spectra recorded on the TM segment SSDPLVVAASIIGILHLILWILDRL reconstituted in DMPC reveal a similar tilt of $31.6 \pm 6.2^\circ$ [88]. Results from substituted cysteine accessibility on the TM segment (25–44) transcribed in oocytes suggest that the M2 has a funnel-like structure with its wider end towards the cytoplasmic side [89].

CD spectroscopy has been used to assess the secondary structure of the TM domain of NB in methanol and reconstituted in POPC [75] (Table 1). Quantitative analysis of the data for NB reconstituted in vesicles reveal ca. 65% of helix structure. The double minimum at 208 and 222 nm usually found for helix structure is merged to a single minimum at 220 nm with a shoulder at ca. 230 nm. However, the maximum at 195 nm is typical for helix structure regarding its position and height. According to the overall similarity of NB with M2 a helical motive for crossing the lipid membrane is most likely. Further studies have to be done to characterise the reason for the ‘low’ helix content.

Polarised FTIR spectroscopy with a putative TM segment of CM2 (ENQG⁵⁰YMLTLASLGL⁶⁰GIITMLYLLV⁷⁰KIIE) isotopic labelled ($1\text{-}^{13}\text{C}$) at positions Gly59/Leu66 and Gly61/Leu68 reveal a tilt angle of the helices of $(14.6 \pm 3.0)^\circ$ [90] (Table 1). The rotational pitch angle is calculated to be $(218 \pm 17)^\circ$. Assuming a pentameric assembly a global MD search protocol [91] including the data mentioned is run. The ‘best’ bundle structure is a left handed coiled coil with a crossing angle of ca. 16° . In this structure the pore seems to be occluded by Leu⁵⁵ and Met⁶⁵. Hydrogen/deuterium exchange studies using the amide II band as reference show that 34% of the peptide is accessible to deuterium. This result is interpreted as a TM part of 19–20 residues which should be buried in the membrane.

The first evidence of the helical motive of the TM segment of Vpu emerge from CD spectroscopy on Vpu^{1–39} in trifluoroethanol (TFE) [92]. The helical structure of the TM domain is now also confirmed by NMR [93] and FTIR [94] spectroscopy (Table 1). NMR and FTIR spectroscopy reveal small tilt angles of $< 30^\circ$ (NMR) and $\sim 6.5^\circ$ (FTIR). The discrepancy between the NMR and FTIR data might be explained by the fact that the sample for the FTIR spectra had been dried, obtaining lipids in the gel phase, while the solid state NMR spectroscopic data are recorded with the lipid/peptide composition dried on small cover glass and rehumidified to ca. 93% relative humidity. For the solid state NMR spectroscopic data samples with single isotope labelled TM domains of Vpu oriented in lipid membranes had been recorded. A combination of solution and solid state NMR with uniformly ^{15}N labelled full length Vpu and fragments such as Vpu_{2–51} and Vpu_{28–81} reveal tilt angles for the TM segment of $\sim 15^\circ$ and orientation of Vpu_{28–81} parallel to the membrane surface [95]. Full length Vpu and the individual fragments are expressed in *E. coli* and then reconstituted in micelles or lipid bilayers in this study.

In 1995, the first attempt was made to elucidate the structure of the cytoplasmic domain [92]. Nine short segments consisting of 15 amino acids corresponding to a sequence of the cytoplasmic domain (residues 28 to 81) were synthesised by solid phase peptide synthesis. Starting with a segment Vpu_{28–42} this window of 15 amino acids was ‘moved’ towards

the C terminus resulting finally in the peptide Vpu_{67–81}. The analysis of the CD spectra of each of these segments recorded in a mixture of TFE and water proposed substantial helicity for each segment. In combination with ¹H NMR spectra it was suggested that Vpu adopts a helical structure from residue 42 to 50 and from residue 57 to 69. These helices and their position have been refined in later studies by the same authors suggesting a helix–flexible-helix–turn motive with helices at positions Lys-37 to Asp-51 and Glu-57 to His-72 [96]. Another group recorded NMR spectra of a peptide corresponding to the complete cytoplasmic domain in aqueous solution with high salt concentration [97]. Helices are suggested to extend from positions Asp-40 to Ala-50 and Asp-60 to Val-68. A shorter helix from Pro-75 to Asp-79 was also found.

Solid state NMR experiments with single isotope labelled Vpu ([¹⁵N-Leu45]Vpu_{27–57}) with and without phosphorylation at the two serines 52 and 56 do not show any major impact of phosphorylation on helix orientation of this segment [98]. However, signal distribution for the phosphorylated peptide accounts for a broad range of different orientations. This can be best explained by a weakened association of the segment with the membrane. Segments with Vpu close to its C-terminal end ([¹⁵N-Ala62]Vpu_{51–81}) show large ¹⁵N chemical shift anisotropy. This indicates that there is no specific alignment with the membrane. Synchrotron X-ray reflectivity data suggest similar orientation of parts of Vpu on a membrane surface [99]. Also, parts of the protein are aligned parallel to the membrane normal. Low surface pressure seems to be in favour of the TM part of the protein being within the lipid environment whereas the cytoplasmic domain seems to have no contact with the membrane. At higher surface pressures part of the cytoplasmic tail orients parallel to the membrane surface.

Experimental evidence for the teepee-like structure of Kcv has not yet emerged.

3. Computational analysis: channel structure and possible gating mechanisms

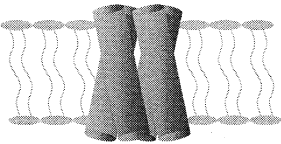
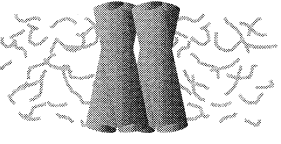

The ‘indirect’ structural data discussed in Section 2 allow us to construct a relatively good ‘low resolu-

tion’ model of particular viral ion channels. However, with the need of a ‘high (atomic) resolution’ structure, computational methods such as MD simulations serve as a link between the two models until the latter is available from experiment. Computational methods will not only allow the visualisation of the results on an atomic scale, but will also let first gentle questions on the role of particular side-chains; the mechanics of the protein, and drug–protein interactions based on the laws of biophysics to be addressed. Once we are in possession of atomic structures from experiments MD simulations will further provide a link from structure to function. The following paragraphs provide an overview of the progress of investigations using computational derived models, and what is needed for the future.

3.1. MD simulations on M2

Simulations with a homotetrameric ensemble of the TM region of M2 (Ac-LVIAASIIIGILHFIL-WIL-NH₂) in a hydrophobic slab of a low dielectricum is conducted in the presence of water molecules [37,100] (Table 2). This region has been found to form a core helical region despite the overall length of the single TM segment [101]. The four helical TM segments are designed to form a left handed super coiled bundle with a tilt angle of 5°. This alignment allows for key residues such as F38, A30, S31, G34, H37, F38, and W41 to be within the pore lumen. The position of these residues is now proved by experimental findings [89]. In this study [89] M2 mutants have been generated in which the residues mentioned have been replaced by cysteines. The accessibility of these cysteine mutants to sulfhydryl-specific reagents (substituted-cysteine accessibility method) was tested using whole cell current measurements. For this oocytes were used as expression system for the M2 mutants. H37 is assumed to act as a gate due to its pK_a of 6.1. As a possible gating mechanism it is proposed that protonation of the histidines induce a kind of ring flipping (model I) [102] (Fig. 2). With the pyrrole rings aligned perpendicular to the membrane surface protonation on one of the nitrogen atoms induce a rotational motion thereby moving the proton to the high pH side. Models with all four histidines protonated and unprotonated are constructed to represent the open and closed state,

Table 2
Simulations performed on the viral ion channel proteins

	M2	NB	CM2	Vpu	Kcv
 Hydrated lipid bilayer	Single helix [101], bundle of 4 helices [101, 103].	Single helix [110], bundles of 4, 5, and 6 helices [75]	Single helix [110]	Single helix [110], bundle of 5 helices [116]	-
 Octane mimeticum	Bundle of 4 helices [104]	-	-	Bundle of 5 helices [112].	-
 Slab of low dielectricum	Bundle of 4 helices [37, 100]	Bundles of 4, 5, and 6 helices [109]	-	Bundles of 4, 5, and 6 helices [111]	-

respectively (model II) [100]. All models increase their super coiling during a simulation of 1 ns resulting in tilt angles of 20–25°. This allows for a stronger crossing of the helices of up to 35°. Interestingly, the closed state (all four histidines unprotonated) interrupts the continuous water column found for the open state (all histidines protonated). In the latter case the histidines orient towards the helix–helix interface. In a more recent study with a similar model a water-filled ‘cavity’ within the bundle has been revealed [103]. Three water molecules do not appear to exchange with the surrounding waters during the entire duration of the simulation. Simulations (4 ns) of four parallel orientated TM segments (SSDPLVVAASIIGILHLILWILDRL) in the bilayer mimetic octane tend to form similar left handed super coiled structures (tilt angle at the end of the

simulations $27 \pm 5^\circ$) [104] as found in the simulations mentioned [103]. For the ‘closed’ state (histidines unprotonated) water molecules only gradually enter the pore half way through the simulation [104]. The protonation of two histidines forces the histidines to give way to a uniform water column. Simulations with tetrameric bundles of the TM segment of M2 in a bilayer system with two and four of the histidines protonated result in a similar effect on the bundles [105]. Simulations with a tetrameric bundle of the putative TM region of M2 in an octane slab, having one protonated histidine, also show an opening of the bundle and the formation of a water column through the pore [106]. Simulations with a longer TM segment suggest that residues S23 and D24 may also play a role in the gating mechanism of the channel [107] [101]. Investigations of the ionisa-

tion states of the aspartic residues by calculating their pK_a values suggested that only one residue is unprotonated. Also, these bundles seem to remain stable during the simulation in a fully hydrated bilayer (POPC) and allow for a water filled pocket at the C-terminal end of the pore. Simulations of bundles with TM segments of different length (consisting of 18 or 22 amino acids) suggest that the bundle with the shorter segment retains the initial tilt angle better than bundles with longer segments. The effect is attributed to the compensation for hydrophobic mismatch of the bundles with longer segments because of the thickness of the bilayer.

The general feasibility of generating models of TM helical bundles by the assumptions mentioned above is demonstrated in a comparative study of those bundles and bundles built upon experimental constraints [108].

3.2. MD simulation on NB and CM2

For NB the exact number of segments forming a channel is not yet known. Experiments with gels under non-reducing conditions indicate the formation of disulphide-linked dimers and also oligomers [56]. Similarity in the length of NB with M2 and the almost identical life cycles of these viruses suggest that the TM region of NB also adopts a helical structure. Bundles of four, five and six segments according to the putative TM section of NB are generated. They are placed in a hydrophobic slab with a low

dielectricum and restraint MD simulations are applied [109] (Table 2). The super coiling seems to be reduced at the end of the simulation (100 ps). Estimated conductance based on ohmic calculation of an irregular ‘tube’ of electrolyte solution of the same dimension as the interior of the channel including an empirical correction for the lowered mobility of waters in restricted geometries are in agreement with experimental data. Bundles of five segments seem to be the most appropriate model for the NB channel architecture. The stability of the isolated helical TM strands in a fully hydrated lipid bilayer (POPC) is tested with three single TM segments of different lengths (20, 28 and 36 amino acids in length) representing the most likely TM region [110]. Each of the single strands are placed individually into a lipid bilayer (POPC) and the whole system hydrated. Simulations for 1 ns reveal fairly stable segments. Segments of 28 amino acids in length are chosen to form bundles of different size (four, five and six segments) (Fig. 4) [75]. These bundles are also placed in a lipid bilayer and the simulation run for 1 ns. The segments are orientated in such a way that all the hydrophilic residues (serines and threonines) are facing the pore. Calculations of the conductance of a 0.5 M KCl solution based on the pore diameters of the bundles after 1 ns reveal a minimum value of 20 pS for the bundle of four segments. Agreement with the lowest values found in the experiments [75] indicate a bundle as small as the M2 channel from influenza A. The bundles were constructed with no

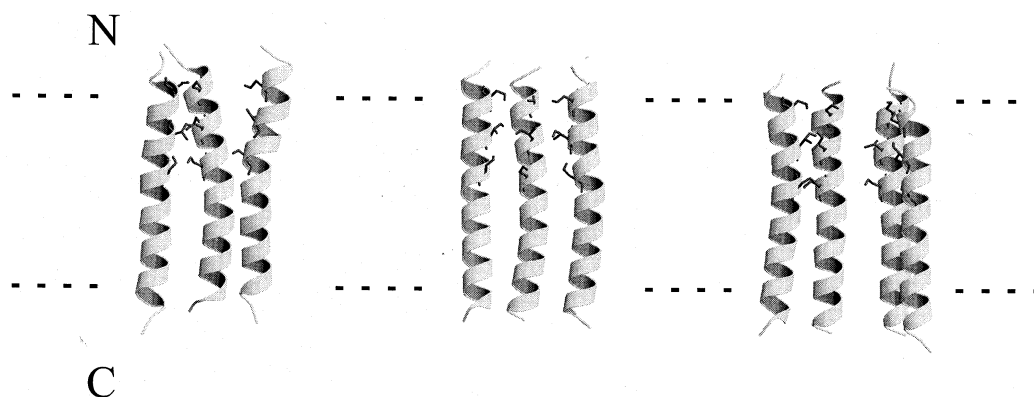


Fig. 4. Bundle of four (left), five (middle) and six segments (right) of NB after 1 ns simulation in a fully hydrated lipid bilayer. To see inside the bundle one segment of the bundle-4 is omitted for clarity. Two segments in each bundle-5 and bundle-6 are removed. Serines and threonines are shown in stick modus (dark grey). Not shown are lipid bilayer and the water molecules present in the simulation. N- and C-terminal ends are indicated. The dashed line indicates the boundaries of the lipid bilayer. Graphs were generated using MOLSCRIPT.

initial tilt angle. At the end of the simulation there is a trend of a decreasing tilt angle with increasing numbers of segments. The position of the side-chain remain stable during the simulation.

For CM2 similar calculations with single helical TM segments are undertaken [110] (Table 2). Similar to NB and Vpu the strands remain their helicity. The subsequent assembly of the strand with 28 amino acids give rise to stable bundles as well. However, residues such as lysine and glutamic acid form salt bridges at the C-terminal of the pores of the CM2 bundles (Fischer and Sansom, unpublished results).

3.3. MD simulations on Vpu and Kcv

Vpu: two approaches are undertaken to perform modelling and simulation studies on the TM segment of Vpu [111,112] (Table 2). In an investigation of assembled TM domains of Vpu (IVAIVA¹⁰LVVAIIIAIV²⁰VWSIVII) by Sansom et al. [111] bundles consisting of four, five and six helices per bundle are generated. In these bundles the serines are placed towards the interior of the bundle. Simulations are performed with the bundles placed in an artificial bilayer represented by a hydrophobic slab and with restraints regarding the helicity of the bundles and their assembly. Water molecules are also constrained to remain within the mouth of the bundle during the simulation. Potential energy profiles for ion/channel interactions support the experimental finding of a weak cation selectivity over anion selectivity.

Calculation of the conductance and comparison with experimental results suggest that the most plausible bundle structure would be a pentameric assembly.

In a second approach, simulations (1 ns) of two hydrated pentameric bundles embedded in octane, a bilayer mimic, have been performed without any restraints on the peptide helices [112]. The same TM sequence is used as in Grice et al. [111]. One of the model is built according to the model of Grice et al. [111] in which all serines are facing the lumen of the pore. A second model is built placing all the tryptophans explicitly so that they face the pore. Both structural models have in common (i) an orientation of the tryptophans towards the helix/helix and helix/lipid interface, and (ii) the disappearance of a continuous water column within the bundle. All bundles adopt a conical shape with a water-filled pocket towards the C-terminal end. The data are interpreted in terms of a non-ion-conducting pore. An average tilt angle of the segments with respect to the octane normal was calculated to be 4.2° [113].

FTIR spectroscopic data in combination with globular MD support a pentameric TM bundle (MQPIQIAIVA¹⁰LVVAIIIAVV²⁰WSIVIIIEYRK) with all tryptophans pointing into the pore [114]. This bundle structure is interpreted as a potential ‘closed’ structure of the channel. In contrast, models with the tryptophans at the helix–lipid headgroup interface might represent an ‘open’ structure [111]. Simulations in a fully hydrated lipid bilayer (POPC)

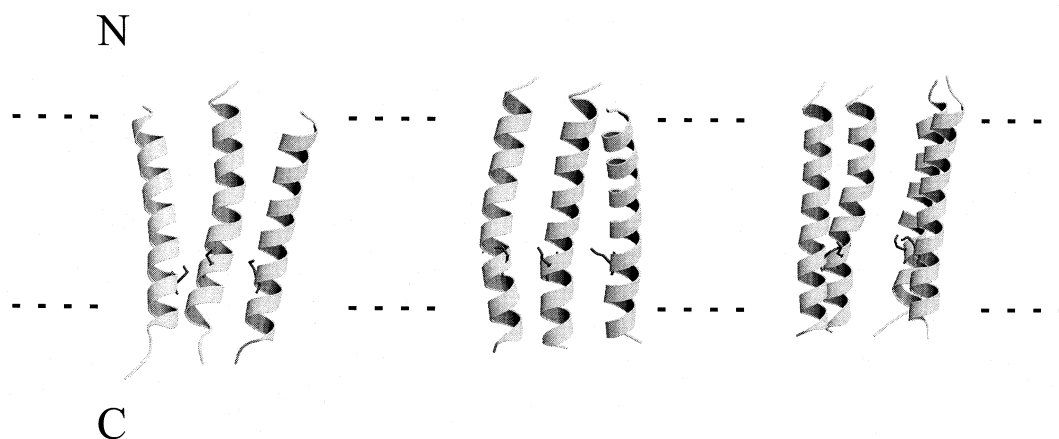


Fig. 5. Bundle of four (left), five (middle) and six segments (right) of Vpu after 1 ns simulation. Description as in Fig. 4. Serines are shown in stick modus (dark grey).

were undertaken with (i) one model from Arkin et al. [114], (ii) an equivalent model built *in silico* using a combined Xplor and SA/MD approach [115,116], and (iii) model with serines facing the pore [116]. For models (i) and (iii) tryptophans in all segments move towards the helix/helix interface during the simulations. In the case of model (ii) all tryptophans remain in the pore. In conclusion, it is possible that gating is *via* a rotational-like motion of the segments, rather than the incorporation or omission of another segment to or from the existing circular assembly. Such a ‘screw-like’ motion would block the channel by exposing hydrophobic residues to the pore and creating a dielectric barrier which cannot be passed by ions. A similar barrier is proposed to exist in the nicotinic acetylcholine receptor [117].

Simulations were also performed on extended TM segments (28 amino acids) forming bundles of four, five and six segments embedded in a hydrated lipid bilayer (Fig. 5) generated as mentioned for NB. Focussing on particular side-chains such as arginines indicate that these residues point into the pore, literally occluding the pore (Cordes, Sansom, Fischer, to be published). Since Vpu shows channel activity, the model might reflect only a ‘snapshot’ of possible orientations of these residues *in vivo*. Thus, inclusion of the extramembraneous parts of Vpu in the simulation studies are essential. This makes the need of a high-resolution structure of complete Vpu and, of course, the other viral channel proteins obvious.

For Kcv no simulations have yet been performed.

3.4. Expectations for the future

We are still missing detailed structural data of the full length membrane proteins. All simulation and most of the spectroscopic analysis has up to now mostly been done with peptides analogous to the TM segments. It is probable that the extramembraneous and cytoplasmic segments affect tilt angles of the TM segments and therefore the orientation of essential side-chains (e.g. histidines in M2). Simulation on larger systems is already possible. Thus, the next step in simulations should be to include the non-TM parts as best as possible. Simulations on bundles of these larger single segments will of course be of further interest.

4. Channel–drug interaction

Channel activity of M2 is inhibited by amantadine (1-aminoadamantane hydrochloride) [118] and rimantadine (α -methyl-1-adamantane methylamine hydrochloride) (for reviews see [119–122]). Above 0.1 mM amantadine effects the membrane fusion activity of haemagglutinin during endocytosis ([38] and references therein). However, this effect is not restricted to amantadine but also can also be found with other compounds such as amines. Also the development of other enveloped viruses such as influenza B and some RNA viruses can be inhibited in this concentration range. Concentrations between 0.1 and 5 μ M, however, exhibit strain-specific inhibition during the entry of the virus and its assembly in the later part of the life cycle. Amantadine-resistant strains from Singapore, Rostock, and Weybridge have mutations at positions 27, 30, 31 and 34. They are located in the putative TM region of the channel protein M2 [38]. Single channel recordings with a synthetic analogue of the TM region of M2 show that exactly this segment is responsible for channel blocking with amantadine in a concentration of 20 μ M [21]. The efficiency of M2 inhibition by ca. 100 μ M follows the sequence of the virus strands Udorn > Weybridge > Rostock [22]. The Weybridge strain is characterised by several mutations from which two are within the TM region of M2. To test whether the TM region is responsible for the sequence of efficiency mutations of the Rostock strand at I-27-V and L-38-F are produced. Analysis with either a I-27-V or a L-38-F single residue mutant reveal that the former mutation can more easily be blocked by amantadine. The amantadine block of M2 protein expressed in oocytes of *X. laevis* is irreversible [22]. If M2 protein is expressed (in either *S. frugiperda* or in influenza A infected CV-1 cells), purified, and reconstituted into lipid bilayers, recordings in the presence of amantadine show reduced probability of opening [66]. Also M2 channel is less often in its most probable conductance state. Amantadine blocks M2 in its tetrameric form [72]. Investigations of the TM segment of M2 in DPC in the presence of amantadine by analytical ultracentrifugation indicate that the peptide tends to be in the tetrameric state. The results are interpreted in the terms of amantadine competing with the protons for binding to deprotonated histi-

dines in the tetramer. Whole cell current measurements of M2 expressed in oocytes of *X. laevis* in the presence of Cu(II) inhibit channel activity [123]. Two different binding sites for Cu(II) are found, one site with low binding specificity and one site with high affinity. The type of interaction and the induced current behaviour for Cu(II) binding to the latter site seems to be similar to the inhibition of amantadine. Since mutations of His-37 by alanine or glycine eliminates binding at the high affinity site, these results have been taken as a further support for the location of the amantadine binding site within the TM region of M2.

NB channel activity is also affected by the presence of amantadine. Bilayer experiments of NB transcribed in *E. coli* and reconstituted into the lipid bilayer (palmitoyl-oleoyl-phosphatidylethanolamine, palmitoyl-oleoyl-phosphatidylserine and palmitoyl-oleoyl-phosphatidylcholine, 5:3:2) indicate lower and less frequent currents in the presence of the anti-viral drug [74]. However, the concentration of amantadine necessary for these findings is several orders of magnitude higher (ca. 2 mM) than those effecting M2 (0.1–5 μ M). Experiments with solely the TM segment of NB reconstituted in POPC show similar current behaviour at the lower drug concentration of around 0.04–0.06 mM [124].

Whether amantadine affects channel activity by simply blocking the pore or via allosteric coupling is not yet fully understood. Experiments support the latter type of blocking [66]: (i) inhibition is more favoured in the open state, (ii) there is a reduced mean current in the presence of amantadine, and (iii) there is no rectification in the presence of charged amantadine. Neutron diffraction experiments with amantadine in the presence of lipids show that amantadine penetrates into the lipid membrane and interacts with M2 at specific sites [125]. Amantadine is found around 5 Å from the centre of the bilayer. This suggests an interaction site with Val-27 and Ser-31. A steric block within the channel is suggested. Computational methods reveal a minimum in the energy profile along the pore axis for amantadine in this region [100].

Kcv is blocked with a three orders of magnitude higher amount of amantadine than M2 [16]. The inhibition is voltage independent and can be reversed within minutes of amantadine removal. These results

suggest that the inhibition of Kcv induced by amantadine is different from the inhibition of M2.

A spirene-containing compound BL-1743 (2-[3-azaspiro (5,5)undecanol]-2-imidazoline) has been also found to affect virus growth [39] by blocking channel activity of M2 [40]. A virus strand with a mutation I-35 to T is by far more resistant (> 70-fold) to BL-1743 than to amantadine. This suggests that the drug–protein interaction is different for these two drugs.

Several derivatives of amantadine have been synthesised [42] and tested for anti-viral activity using protocols which are described by De Clerq et al. [126–128]. Spiro piperidine- and spiro morpholine-amantadine with a six-membered heterocyclic ring and molecules with a rimantadine body and pyrrolidine rest show high potency against influenza A if the valency of the nitrogens is satisfied with hydrogen atoms. The same molecules are active against influenza B as well, albeit in higher concentrations. If the nitrogen is connected with aliphatic rests, potency against HIV-1 rises, but not yet sufficient to give a major breakthrough.

5. Conclusion and outlook

In recent years there is a relatively clear picture evolving regarding the structure and function of, in particular, two channels: M2 from influenza A and Vpu from HIV-1. It is accepted that M2 is a proton conducting disulphide-linked homotetrameric proton channel. The protein spans the lipid bilayer via an α -helix. Its conductance can be selectively blocked by amantadine which forms the basis of its anti-viral use. Vpu seems most likely to form a homopentameric assembly with helical TM segments. Ion conductance is suggestive and preferentially of cations. Whether channel activity is the *in vivo* source of its functioning is, however, still being debated. Also no channel blocking of amantadine is observed which might question the formation of ‘real’ channels. Vpu is the only channel for which we have suggestions for the structure of the extramembraneous part. Channel activity for NB protein has been found as well as experimental evidence that the TM segment forms an α -helix. Ion conductance and ion preference is dependent upon the experimental conditions.

The number of proteins needed to assemble to form a proper channel can only be speculated; it might range from four to six units. Less is known about CM2. FTIR spectroscopic data suggests a helical motive for the TM spanning part, however, channel activity still has not been demonstrated either in cells or with protein or peptide reconstituted into lipid bilayers. Kcv's structure is suggested according to the homology of its sequence to the TM part of the K⁺-channel proteins.

Despite all experimental evidence for ion channel activity of NB protein, Kcv and Vpu protein, our knowledge about channel activity might still be a consequence of the expression of these membrane proteins in particular cells. Unless a selective blocker is found for these proteins and tested in cell systems, the term 'ion channel' has still to be used with some caution (see [77] for a thorough assessment of this topic). However, the most recent results on Vpu regarding selective blocking of channel activity are in favour of Vpu as an ion channel forming protein (Ewart et al., early online publication in *Eur. Biophys. J.* (2001), <http://link.springer.de/link/service/journals/00249/tocs.htm>).

For M2 it is found that the protonation state of the histidines is essential for gating. Protonation of the histidines would force them either to rotate or to move apart from each other caused by electrostatic repulsion. In the latter case this would go in concert with a rotational like motion of the helices. For Vpu a similar gating mechanism looks likely. Twist like rotational motions of parts of the TM segments has been suggested for more complex ion channels like the nAChR [117]. For the Na⁺-channels a 'screw-like' motion is predicted for the TM voltage sensor (S4) of the channel upon a high transmembrane potential [129–131]. The viral ion channels seem to use similar mechanisms for gating albeit their minimalist design.

We are still at the beginning of understanding the viral ion channels on a structural level. Detailed high resolution structural data are urgently required to allow the application of computational based methods for the investigation of drug–protein interaction. In parallel more information about the role of these membrane proteins in the life cycle of the virus is essential. The viral membrane proteins are an extremely interesting target to study membrane protein activity on a minimalist design. This might also stim-

ulate the design of novel synthetic channel forming compounds.

In addition, the discovery of the Kcv channel in plant viruses also gives us a glimpse of the kind of viral ion channel we still might find in other viral genomes.

Acknowledgements

W.B.F. thanks the European Commission for financial support (TMR-Fellowship). We further acknowledge helpful discussions with L.R. Forrest and G.R. Smith.

References

- [1] B. Hille, *Ionic Channels of excitable Membranes*, 2nd edn., Sinauer Associates, Sunderland, MA, 1992.
- [2] G.A. Woolley, B.A. Wallace, *J. Membr. Biol.* 129 (1992) 109–136.
- [3] M. Noda, H. Takahashi, T. Tanabe, M. Toyosato, Y. Furutani, T. Hirose, M. Asai, S. Inayama, T. Miyata, S. Numa, *Nature* 299 (1982) 793–797.
- [4] M. Noda, H. Takahashi, T. Tanabe, M. Toyosato, S. Kikuyotani, T. Hirose, M. Asai, H. Takashima, S. Inayama, T. Miyata, S. Numa, *Nature* 301 (1983) 251–255.
- [5] M. Noda, H. Takahashi, T. Tanabe, M. Toyosato, S. Kikuyotani, Y. Furutani, T. Hirose, H. Takashima, S. Inayama, T. Miyata, S. Numa, *Nature* 302 (1983) 528–532.
- [6] A. Devillers-Thiery, J. Giraudat, M. Bentaboulet, J.P. Changeux, *Proc. Natl. Acad. Sci. USA* 80 (1983) 2067–2071.
- [7] T. Claudio, M. Ballivet, J. Patrick, S. Heinemann, *Proc. Natl. Acad. Sci. USA* 80 (1983) 1111–1115.
- [8] G. Winter, S. Fields, *Nucleic Acids Res.* 8 (1980) 1965–1974.
- [9] H. Allen, J. McCauley, M. Waterfield, M. Gething, *Virology* 107 (1980) 548–551.
- [10] R.A. Lamb, C.-J. Lai, P.W. Choppin, *Proc. Natl. Acad. Sci. USA* 78 (1981) 4170–4174.
- [11] M.W. Shaw, R.A. Lamb, B.W. Erickson, D.J. Briedis, P.W. Choppin, *Proc. Natl. Acad. Sci. USA* 79 (1982) 6817–6821.
- [12] M.W. Shaw, P.W. Choppin, R.A. Lamb, *Proc. Natl. Acad. Sci. USA* 80 (1983) 4879–4883.
- [13] S. Hongo, K. Sugawara, H. Nishimura, Y. Muraki, F. Kitame, K. Nakamura, *J. Gen. Virol.* 75 (1994) 3503–3510.
- [14] K. Strebel, T. Klimkait, M.A. Martin, *Science* 241 (1988) 1221–1223.
- [15] E.A. Cohen, E.F. Terwilliger, J.G. Sodroski, W.A. Haseltine, *Nature* 334 (1988) 532–534.
- [16] B. Plugge, S. Gazzarrini, M. Nelson, R. Cerana, J.L. Van Etten, C. Derst, D. DiFrancesco, A. Moroni, G. Thiel, *Science* 287 (2000) 1641–1644.

- [17] J.J. Skehel, P.M. Bayley, E.B. Brown, S.R. Martin, M.D. Waterfield, J.M. White, I.A. Wilson, D.C. Wiley, *Proc. Natl. Acad. Sci. USA* 79 (1982) 968–972.
- [18] R.A. Lamb, S.L. Zebedee, C.D. Richardson, *Cell* 40 (1985) 627–633.
- [19] L.J. Holsinger, R.A. Lamb, *Virology* 183 (1991) 32–43.
- [20] R.J. Sugrue, A.J. Hay, *Virology* 180 (1991) 617–624.
- [21] K.C. Duff, R.H. Ashley, *Virology* 190 (1992) 485–489.
- [22] C. Wang, K. Takeuchi, L.H. Pinto, R.A. Lamb, *J. Virol.* 67 (1993) 5585–5594.
- [23] R.J. Sugrue, A.J. Hay, *Virology* 180 (1991) 617–624.
- [24] R.J. Sugrue, G. Bahadur, M.C. Zambon, M. Hall-Smith, A.R. Douglas, A.J. Hay, *EMBO J.* 9 (1990) 3469–3476.
- [25] T. Betakova, M.V. Nermut, A.J. Hay, *J. Gen. Virol.* 77 (1996) 2689–2694.
- [26] D.L. Brassard, G.P. Leser, R.A. Lamb, *Virology* 220 (1996) 350–360.
- [27] K. Strebel, T. Klimkait, F. Maldarelli, M.A. Martin, *J. Virol.* 63 (1989) 3784–3791.
- [28] R.L. Willey, F. Maldarelli, M.A. Martin, K. Strebel, *J. Virol.* 66 (1992) 7193–7200.
- [29] U. Schubert, A.V. Ferrer-Montiel, M. Oblatt-Montal, P. Henklein, K. Strebel, M. Montal, *FEBS Lett.* 398 (1996) 12–18.
- [30] S. Bour, U. Schubert, K. Strebel, *J. Virol.* 69 (1995) 1510–1520.
- [31] U. Schubert, S. Bour, A.V. Ferrer-Montiel, M. Montal, F. Maldarelli, K. Strebel, *J. Virol.* 70 (1996) 809–819.
- [32] M. Paul, S. Mazumder, N. Raja, M.A. Jabbar, *J. Virol.* 72 (1998) 1270–1279.
- [33] T. Kerkau, I. Bacik, J.R. Bennink, J.W. Yewdell, T. Hunig, A. Schimpl, U. Schubert, *J. Exp. Med.* 185 (1997) 1295–1305.
- [34] N. Unwin, *J. Mol. Biol.* 229 (1993) 1101–1124.
- [35] C. Wang, R.A. Lamb, L.H. Pinto, *Biophys. J.* 69 (1995) 1363–1371.
- [36] L.H. Pinto, R.A. Lamb, *Trends Microbiol.* 3 (1995) 271.
- [37] M.S.P. Sansom, I.D. Kerr, S.G. R., H.S. Son, *Virology* 233 (1997) 163–173.
- [38] A.J. Hay, A.J. Wolstenholme, J.J. Skehel, M.H. Smith, *EMBO J.* 4 (1985) 3021–3024.
- [39] S. Kurtz, G. Luo, K.M. Hahnenberger, C. Brooks, O. Gecha, K. Ingalls, K.I. Numata, M. Krystal, *Antimicrob. Agents Chemother.* 39 (1995) 2204–2209.
- [40] Q. Tu, L.H. Pinto, G. Luo, M.A. Shaughnessy, D. Mullaney, S. Kurtz, M. Krystal, R.A. Lamb, *J. Virol.* 70 (1996) 4246–4252.
- [41] I.V. Chizhnikov, F.M. Geraghty, D.C. Ogden, A. Hayhurst, M. Antoniou, A.J. Hay, *J. Physiol.* 494 (1996) 329–336.
- [42] N. Kolocouris, A. Kolocouris, G.B. Foscolos, G. Fytas, J. Neyts, E. Padalko, J. Balzarini, R. Snoeck, G. Andrei, E. De Clercq, *J. Med. Chem.* 39 (1996) 3307–3318.
- [43] D.A. Declan, J.M. Cabral, R.A. Pfuetzner, A. Kuo, J.M. Gulbis, S.L. Cohen, B.T. Chait, R. MacKinnon, *Science* 280 (1998) 69–77.
- [44] v. Heijne, *Biochim. Biophys. Acta* 947 (1988) 307–333.
- [45] G.D. Parks, R.A. Lamb, *Cell* 64 (1991) 777–787.
- [46] R.A. Lamb, S.L. Zebedee, C.D. Richardson, *Cell* 40 (1985) 627–633.
- [47] S.L. Zebedee, R.A. Lamb, *J. Virol.* 62 (1988) 2762–2772.
- [48] R.A. Lamb, P.W. Choppin, *Virology* 112 (1981) 729–737.
- [49] L.J. Holsinger, A. Shaughnessy, A. Micko, L.H. Pinto, R.A. Lamb, *J. Virol.* 69 (1995) 1219–1225.
- [50] R.J. Sugrue, R.B. Belshe, A.J. Hay, *Virology* 179 (1990) 51–56.
- [51] M. Veit, H.-D. Klenk, A. Kendal, R. Rott, *Virology* 184 (1991) 227–234.
- [52] C. Schroeder, C.M. Ford, S.A. Wharton, A.J. Hay, *J. Gen. Virol.* 75 (1994) 3477–3484.
- [53] T. Sakaguchi, Q.A. Tu, L.H. Pinto, R.A. Lamb, *Proc. Natl. Acad. Sci. USA* 94 (1997) 5000–5005.
- [54] R. MacKinnon, *Nature* 350 (1991) 232–235.
- [55] M.A. Williams, R.A. Lamb, *Mol. Cell. Biol.* 8 (1988) 1186–1196.
- [56] M.A. Williams, R.A. Lamb, *Mol. Cell. Biol.* 6 (1986) 4317–4328.
- [57] A. Pekosz, R.A. Lamb, *Virology* 237 (1997) 439–451.
- [58] S. Hongo, K. Sugawara, Y. Muraki, Y. Matsuzaki, E. Takashita, F. Kitame, K. Nakamura, *J. Virol.* 73 (1999) 46–50.
- [59] A. Pekosz, R.A. Lamb, *J. Virol.* 74 (2000) 10480–10488.
- [60] S. Hongo, K. Sugawara, Y. Muraki, F. Kitame, K. Nakamura, *J. Virol.* 71 (1997) 2786–2792.
- [61] F. Maldarelli, M.Y. Chen, R.L. Willey, K. Strebel, *J. Virol.* 67 (1993) 5056–5061.
- [62] U. Schubert, T. Schneider, P. Henklein, K. Hoffmann, E. Berthold, H. Hauser, G. Pauli, T. Porstmann, *Eur. J. Biochem.* 204 (1992) 875–883.
- [63] U. Schubert, P. Henklein, B. Boldyreff, E. Wingender, K. Strebel, T. Porstmann, *J. Mol. Biol.* 236 (1994) 16–25.
- [64] L.J. Holsinger, D. Nichani, L.H. Pinto, R.A. Lamb, *J. Virol.* 68 (1994) 1551–1563.
- [65] C. Wang, R.A. Lamb, L.H. Pinto, *Virology* 205 (1994) 133–140.
- [66] M.T. Tosteson, L.H. Pinto, L.J. Holsinger, R.A. Lamb, *J. Membr. Biol.* 142 (1994) 117–126.
- [67] T. Lin, C. Schroeder, *J. Virol.* 75 (2001) 3647–3656.
- [68] K. Shimbo, D.L. Brassard, R.A. Lamb, L.H. Pinto, *Biophys. J.* 70 (1996) 1335–1346.
- [69] J.A. Mould, H.-C. Li, C.S. Dudlak, J.D. Lear, A. Pekosz, R.A. Lamb, L.H. Pinto, *J. Biol. Chem.* 275 (2000) 8592–8599.
- [70] J.A. Mould, J.E. Drury, S.M. Frings, U.B. Kaupp, A. Pekosz, R.A. Lamb, L.H. Pinto, *J. Biol. Chem.* 275 (2000) 31038–31050.
- [71] G.G. Kochendörfer, D. Salom, J.D. Lear, R. Wilk-Orescan, S.B.H. Kent, W.F. DeGrado, *Biochemistry* 38 (1999) 11905–11913.
- [72] D. Salom, B.R. Hill, J.D. Lear, W.F. DeGrado, *Biochemistry* 39 (2000) 14160–14170.
- [73] K. Tobler, M.L. Kelly, L.H. Pinto, R.A. Lamb, *J. Virol.* 73 (1999) 9695–9701.

- [74] N.A. Sunstrom, L.S. Prekumar, A. Prekumar, G. Ewart, G.B. Cox, P.W. Gage, *J. Membr. Biol.* 150 (1996) 127–132.
- [75] W.B. Fischer, M. Pitkeathly, B.A. Wallace, L.R. Forrest, M.S.P. Sansom, *Biochemistry* 39 (2000) 12708–12716.
- [76] G.D. Ewart, T. Sutherland, P.W. Gage, G.B. Cox, *J. Virol.* 70 (1996) 7108–7115.
- [77] M.J. Coady, N.G. Daniel, E. Tiganos, B. Allain, J. Friberg, J.-Y. Lapointe, E.A. Cohen, *Virology* 244 (1998) 39–49.
- [78] R.A. Lamb, L.H. Pinto, *Virology* 229 (1997) 1–11.
- [79] J.E. Fitton, A. Dell, W.V. Shaw, *FEBS Lett.* 115 (1980) 209–212.
- [80] I.R. Mellor, D.H. Thomas, M.S.P. Sansom, *Biochim. Biophys. Acta.* 942 (1988) 280–294.
- [81] J.D. Lear, Z.R. Wasserman, W.F. DeGrado, *Science* 240 (1988) 1177–1181.
- [82] W. Hanke, G. Boheim, *Biochim. Biophys. Acta.* 596 (1980) 456–462.
- [83] M.S.P. Sansom, *Prog. Biophys. Mol. Biol.* 55 (1991) 139–236.
- [84] K.C. Duff, S.M. Kelly, N.C. Price, J.P. Bradshaw, *FEBS Lett.* 311 (1992) 256–258.
- [85] F.A. Kovacs, T.A. Cross, *Biophys. J.* 73 (1997) 2511–2517.
- [86] F.A. Kovacs, J.K. Denny, Z. Song, J.R. Quine, T.A. Cross, *J. Mol. Biol.* 295 (2000) 117–125.
- [87] Z. Song, F.A. Kovacs, J. Wang, J.K. Denny, S.C. Shekar, J.R. Quine, T.A. Cross, *Biophys. J.* 79 (2000) 767–775.
- [88] A. Kukol, P.D. Adams, L.M. Rice, B.A. T, I.T. Arkin, *J. Mol. Biol.* 286 (1999) 951–962.
- [89] K. Shuck, R. Lamb, L.H. Pinto, *J. Virol.* 74 (2000) 7755–7761.
- [90] A. Kukol, I.T. Arkin, *J. Biol. Chem.* 275 (2000) 4225–4229.
- [91] P.D. Adams, I.T. Arkin, D.E. Engelman, A.T. Brunger, *Structural Biol.* 2 (1995) 154–162.
- [92] V. Wray, T. Federau, P. Henklein, S. Klabunde, O. Kunert, D. Schomburg, U. Schubert, *Int. J. Peptide Protein Res.* 45 (1995) 35–43.
- [93] V. Wray, R. Kinder, T. Federau, P. Henklein, B. Bechinger, U. Schubert, *Biochemistry* 38 (1999) 5272–5282.
- [94] A. Kukol, P.D. Adams, L.M. Rice, A.T. Brünger, I.T. Arkin, *J. Mol. Biol.* 286 (1999) 951–962.
- [95] F.M. Marassi, C. Ma, H. Gratkowski, S.K. Straus, K. Strelbel, M. Oblatt-Montal, M. Montal, S.J. Opella, *Proc. Natl. Acad. Sci. USA* 96 (1999) 14336–14341.
- [96] T. Federau, U. Schubert, J. Floßdorf, P. Henklein, D. Schomburg, V. Wray, *Int. J. Peptide Protein Res.* 47 (1996) 297–310.
- [97] D. Willbold, S. Hoffmann, P. Rösch, *Eur. J. Biochem.* 245 (1997) 581–588.
- [98] P. Henklein, R. Kinder, U. Schubert, B. Bechinger, *FEBS Lett.* 482 (2000) 220–224.
- [99] S. Zheng, J. Strzalka, C. Ma, S.J. Opella, B.M. Ocko, J.K. Blasie, *Biophys. J.* 80 (2001) 1837–1850.
- [100] M.S.P. Sansom, I.D. Kerr, *Prot. Eng.* 6 (1993) 65–74.
- [101] L.R. Forrest, D.P. Tieleman, M.S.P. Sansom, *Biophys. J.* 76 (1999) 1886–1896.
- [102] L.H. Pinto, G.R. Dieckmann, C.S. Gandhi, C.G. Papworth, J. Braman, M.A. Shaughnessy, J.D. Lear, R.A. Lamb, W.F. DeGrado, *Proc. Natl. Acad. Sci. USA* 94 (1997) 11301–11306.
- [103] L.R. Forrest, A. Kukol, I.T. Arking, D.P. Tieleman, M.S.P. Sansom, *Biophys. J.* 78 (2000) 55–69.
- [104] Q. Zhong, T. Husslein, P.B. Moore, D.M. Newns, P. Pattanaik, M.L. Klein, *FEBS Lett.* 434 (1998) 265–271.
- [105] K.J. Schweighofer, A. Pohorille, *Biophys. J.* 78 (2000) 150–163.
- [106] Q. Zhong, D.M. Newns, P. Pattanaik, J.D. Lear, M.L. Klein, *FEBS Lett.* 473 (2000) 195–198.
- [107] L.R. Forrest, A. Kukol, I.T. Arkin, D.P. Tieleman, M.S.P. Sansom, *Biophys. J.* 78 (2000) 55–69.
- [108] L.R. Forrest, W.F. DeGrado, G.R. Dieckmann, M.S.P. Sansom, *Folding and Design* 3 (1998) 443–448.
- [109] M.S.P. Sansom, L.R. Forrest, R. Bull, *Bioessays* 20 (1998) 992–1000.
- [110] W.B. Fischer, L.R. Forrest, G.R. Smith, M.S.P. Sansom, *Biopolymers* 53 (2000) 529–538.
- [111] A.L. Grice, I.D. Kerr, M.S.P. Sansom, *FEBS Lett.* 405 (1997) 299–304.
- [112] P.B. Moore, Q. Zhong, T. Husslein, M.L. Klein, *FEBS Lett.* 431 (1998) 143–148.
- [113] P.B. Moore, Q. Zhong, T. Husslein, M.L. Klein, *FEBS Letters* 431 (1998) 143–148.
- [114] A. Kukol, I.T. Arkin, *Biophys. J.* 77 (1999) 1594–1601.
- [115] A.T. Brünger. (1992) X-PLOR Version 3.1. A System for X-ray Crystallography and NMR, Yale University Press, New Haven, Ct.
- [116] F. Cordes, A. Kukol, L.R. Forrest, I.T. Arkin, M.S.P. Sansom, W.B. Fischer, *Biochim. Biophys. Acta* 1512 (2001) 291–298.
- [117] A. Miyazawa, Y. Fujiyoshi, M. Stowell, N. Unwin, *J. Mol. Biol.* 288 (1999) 765–786.
- [118] W.L. Davies, R.R. Grunert, R.F. Haff, J.W. McGahen, E.M. Neumayer, M. Paulshock, J.C. Watts, T.R. Wood, E.C. Hermann, C.E. Hoffmann, *Science* 144 (1964) 862–863.
- [119] J.S. Oxford and A. Galbraith. (1980) *Pharmacol. Ther.* 11.
- [120] R. Dolin, R.C. Reichman, H.P. Madore, R. Maynard, P.N. Linton, J. Webber-Jones, *New Engl. J. Med.* 307 (1982) 580–584.
- [121] A.J. Hay, *Seminars in Virology* 3 (1992) 21–30.
- [122] R.A. Lamb, L.J. Holsinger and L.H. Pinto. (1994) in *Cellular Receptors for Animal Viruses* (E. Wimmer, ed.), pp. 303–321, Cold Spring Harbor Laboratory, Cold Spring Harbor, NY.
- [123] C.S. Gandhi, K. Shuck, J.D. Lear, G.R. Dieckmann, W.F. DeGrado, R.A. Lamb, L.H. Pinto, *J. Biol. Chem.* 274 (1999) 5474–5482.
- [124] W.B. Fischer, M. Pitkeathly, M.S.P. Sansom, *Eur. Biophys. J.* 30 (2001) 416–420.
- [125] K.C. Duff, P.J. Gilchrist, A.M. Saxena, J.P. Bradshaw, *Virology* 202 (1994) 287–293.
- [126] E. DeClercq, A. Holy, I. Rosenberg, T. Sakuma, J. Balzarini, P.C. Maudgal, *Nature* 323 (1986) 464–467.

- [127] J. Balzarini, A. Karlsson, M.J. Perez-Perez, L. Vrang, J. Walbers, H. Zhang, B. Oberg, A.M. Vandamme, M.J. Camarasa, E. DeClercq, *Virology* 192 (1993) 246–253.
- [128] S. Shigeta, K. Konno, T. Yokota, K. Nakamura, E. DeClercq, *Antimicrob. Agents Chemother.* 32 (1988) 906–911.
- [129] C.M. Armstrong, *Physiol. Rev.* 61 (1981) 644–683.
- [130] H.R. Guy, P. Seetharamulu, *Proc. Natl. Acad. Sci. USA* 83 (1986) 508–512.
- [131] C. Armstrong, *Physiol. Rev.* 72 (1992) S5–S13.
- [132] M.S.P. Sansom, L.R. Forrest, R. Bull, *BioEssays* 20 (1998) 992–1000.